Parameter study of an inductively powered railgun

Oliver Liebfried, Paul Frings

***Abstract*—This article deals with the numerical simulation of an inductively powered railgun in order to determine the electrical parameters of the inductive storage of the pulsed power supply. A numerical model was set up and validated by experimental results. A parameter sweep was performed by varying the time constant of the coil, the initial current and the initially stored energy. The results show that the generated pulse shape, and thus the transfer efficiency and electromagnetic forces, strongly depend on the inductance of the storage coil. On the contrary, the dependency on the coil time constant, and thus on the coil volume for a given coil shape and conductor material, is small and can be neglected for high time constants.**

I. INTRODUCTION

There are several reasons why inductive storages are used within a pulsed power generator for railguns. In combination with a homopolar generator or a battery, the inductor is used to generate the high voltage which is needed to supply railguns with high armature velocities [1]–[3]. In capacitor banks, inductors are used to limit the maximum current dI/dt and adjust the pulse length to the requirements of the railgun [4]. In this paper, inductors in combination with batteries are considered to be a viable possibility of optimizing the energy chain [5]. Once the inductor is energized, the final pulse shape and the energy transfer efficiency depend mainly on its electrical parameters and how they are matched to the railgun system. In this work, an electromagnetic railgun powered by an inductive storage is simulated. The parameters of the railgun were chosen according to the experimental values of the existing railguns at ISL and were matched to a system with a muzzle energy of 25 MJ according to [6]. Several parameters like the time constant τ of the coil, the initial current I_0 and the initial stored energy W_0 were varied by performing a parameter sweep in order to find valid coil parameters to accelerate an 8 kg projectile to a muzzle velocity of 2500 m/s by using a 6.4 m long railgun barrel.

Similar investigations of railgun systems were repeatedly performed by other researchers. Recently, Xukun Liu et al. analyzed for example the performance of a railgun system supplied by a pulse forming network with an initial capacitive energy of 1.8 MJ [7]. They optimized the system with respect to the efficiency by varying parameters like the segmentation of the capacitor bank, the trigger times of the single PFUs, the capacitor capacitance and charging voltage, projectile mass and railgun length. However, the inductance per PFU was kept constant. The generic algorithm of MATLAB was used for parameter optimization. Richard T. Meyer et al. maximize efficiency for a given railgun system in dependance of a variable muzzle velocity by means of variable charging voltage and trigger times of a given capacitive pulse forming network. The optimization was performed by using MATLAB's fmincon function [8]. Hundertmark et al. simulated a capacitive power supply for the same railgun artillery scenario as used in this paper [9]. A Pspice circuit to determine the size and trigger times of the PFN was used. The influence of the series resistance of the current conducting path on the railgun performance was shown.

Many more paper are dealing with the parameter optimization of railgun systems. See the introduction of [8] for an overview. Most of them apply numerical algorithms to optimize the effic

II. RAILGUN MODEL

Based on the existing railgun systems at ISL, a conventional railgun which is fed by a charged storage inductor via a single interface at the breech is assumed. According to [10], such a simple railgun system can be described by applying Kirchhoff's circuit law. Hence,

$$\begin{aligned}\Big[L' \cdot \frac{dx(t)}{dt} + R'(x(t)) \cdot x(t) + R_{arm} + R_{coil} + R_w + \\ R_{sw}\Big] \cdot I(t) + [L_{coil} + L_w + L' \cdot x(t)] \cdot \frac{dI(t)}{dt} = 0\end{aligned} \tag{1}$$

where L_{coil} and R_{coil} are the inductance and resistance of the storage coil. L_w and R_w are the corresponding entities for the wire. R_{sw} represents the resistance of the switches. L' and R' are the inductance and the resistance gradients of the railgun, respectively. The variable x is the armature position inside the railgun and R_{Arm} the armature resistance. The propulsion of the projectile results from the force equation

$$F = m \cdot \frac{d^2x(t)}{dt} = \frac{1}{2} \cdot L' \cdot I(t)^2 \cdot (1-\beta) \tag{2}$$

with the projectile mass m and the loss factor β, which is introduced as a simple means of considering mechanical friction losses.

The rail resistance was determined by taking into account the velocity skin effect according to [11] and is written:

$$R'(x) = \frac{16}{3w}\sqrt{\frac{\pi\mu}{2\kappa}}\sqrt[4]{\frac{a}{2x}} \tag{3}$$

with the rail width w, the acceleration a, the permeability μ and the conductivity κ of copper. In a first approach, a constant a was used for the calculation of R'.

O. Liebfried is with the French-German Research Institute of Saint-Louis (ISL), 5 rue Général Cassagnou, 68301 Saint-Louis, France, e-mail: Oliver.Liebfried@isl.eu.

Paul Frings is with the Laboratoire National des Champs Magnétiques Intenses (LNCMI), 143 av. de rangueil, 31400 Toulouse, France, e-mail: paul.frings@lncmi.cnrs.fr.

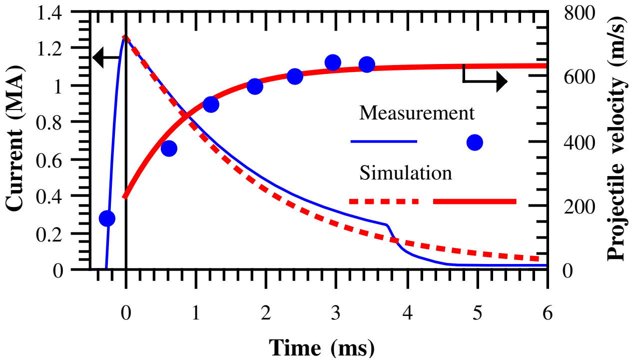

Fig. 1. Simulated and measured data of a railgun shot at ISL

For the parametric study, Wolfram Mathematica was used to numerically solve the equations by applying the following initial conditions

$$I(t=0) = I_0; \quad x(t=0) = x_0; \quad \frac{dx(t=0)}{dt} = v_0. \tag{4}$$

The corresponding Mathematica code was verified by simulating an existing railgun at ISL with satisfactory results (see Fig. 1). In contrast to the simulation used in this parametric study, the railgun is supplied by capacitive pulse-forming units [4]. Its capacitors are discharged into a pulse forming-inductor, coaxial cables and the railgun in series connection. When the current reaches its maximum, the capacitors are discharged and a crowbar diode ensures that the energy stored in the circuit inductances is transferred to the railgun. During this period, the pulse-forming unit acts as an inductive power supply. Therefore, the simulation in Fig. 1 starts at the time instant of the current maximum with I_0, x_0 and v_0, as given by the measurement. Differences between the simulated curves and the measurement occur due to neglecting several physical details like ohmic heating or the skin effect in the cables.

Finally, system parameters taken from [6] for a railgun used as a ship artillery system are applied to the simulation code. Table I recapitulates the system parameters which are used as input for the calculation. The parameters not given in [6] were assumed on the basis of our experience with the railgun systems at ISL.

The parameter study was conducted by numerically solving Eqs. 1 - 3 with varying values for the initial charging energy W_0, the initial current I_0 and the coil time constant τ. The corresponding storage inductance L_{coil} and coil resistance R_{coil} were determined by using the inductive energy formula $W = \frac{1}{2} L \cdot I_0^2$ and the relationship $\tau = L_{coil}/R_{coil}$.

First, τ and W_0 were kept constant. The initial charging current I_0 was varied between 1 and 10 MA within a DO loop. Afterwards, the results were filtered for the condition $v(x = 6.4\,\text{m}) = 2500\,\text{m/s}$. The procedure was repeated for energies ranging from 50 MJ to 125 MJ. Thus, one solution for each energy step was found. In the end, the calculations were repeated for six different values of τ (10 ms, 25 ms, 50 ms, 100 ms, 1 s, 5 s).

TABLE I
SIMULATION INPUT PARAMETERS

Projectile weight	$m = 8\,\text{kg}$
Muzzle velocity goal	$v_{muzzle} = 2500\,\text{m/s}$
Railgun length	$x_{muzzle} = 6.4\,\text{m}$
Rail width	$w = 0.1\,\text{m}$
DC acceleration	$a = 50\,000\,\text{g}$
Inductance gradient	$L' = 0.46\,\mu\text{H/m}$
Wire inductance	$L_w = 26\,\text{nH}$
Wire resistance	$R_w = 68\,\mu\Omega$
Switch resistance	$R_{sw} = 75\,\mu\Omega$
Armature resistance	$R_{arm} = 10\,\mu\Omega$
Storage coil inductance	$L_{coil} = 2W_{coil}/I_0^2 - L_{cable}$
Storage coil resistance	$R_{coil} = L/\tau$
Friction loss factor	$\beta = 0.1$

III. RESULTS

Figure 2 shows the waveforms of the discharge current, the breech voltage, the projectile position, the projectile velocity and the propelling force in respect to time of one exemplary set of input parameters. The current starts at the initial value of 7.9 MA. The initially stored energy in the coil is 66 MJ for this example. The current decreases with a slope down to 2 MA. The curve ends at $t = 3.6\,\text{ms}$. At this time, the projectile reached the end of the railgun(position $x = 6.4\,\text{m}$) with the desired speed of 2500 m/s. This means an energy of 4.6 MJ is still stored in the coil at the end of the acceleration process and can be considered as loss if it is not be recuperated. The voltage increases first due to the speed voltage term in eq. 1 ($L'_{RG} \cdot dx(t)/dt$) and decreases at later times due to the low railgun current. Note, that there is a voltage maximum of about 4 kV which has to be considered when designing the power supply system. The position of the projectile increases according to the increasing velocity. The velocity shows an exponential behavior. There is a steep increase in the beginning and a converges to velocity limit at later times. This behavior is directly linked to the acceleration force, which is proportional to the square of the current as can be concluded from eq. 2. Thus, the maximum acceleration of 15.5 meganewtons appear at the beginning of the discharge process and decrease accordingly.

Figure 3 shows a family of current waveforms for different input energies but a constant τ. A constant τ means that we have a given coil and that we change only the wire section and number of turns in order to change the coil inductance and resistance to match it to the railgun. The projectile can reach the velocity goal with each of the current pulses presented. The red curve is based on a coil inductance of 1.13 µH. The current pulse has a high initial current of 10 MA and a pronounced current decline (-dI/dt). The remaining current in the system after the projectile leaves the bore is as small as 1.6 MA, which is equivalent to a remaining inductive energy of 1.1 MJ. Applying bigger inductances like 8.08 µH (i.e. by reducing the conductor section and making more turns) gives a rather flat current pulse with a much smaller current peak (see blue waveform) but with a magnetic energy of 59 MJ stored in the system inductances after the projectile has left the bore. In this case, the initial energy is 125 MJ. If the remaining energy is considered to be lost, the transfer efficiency can be calculated

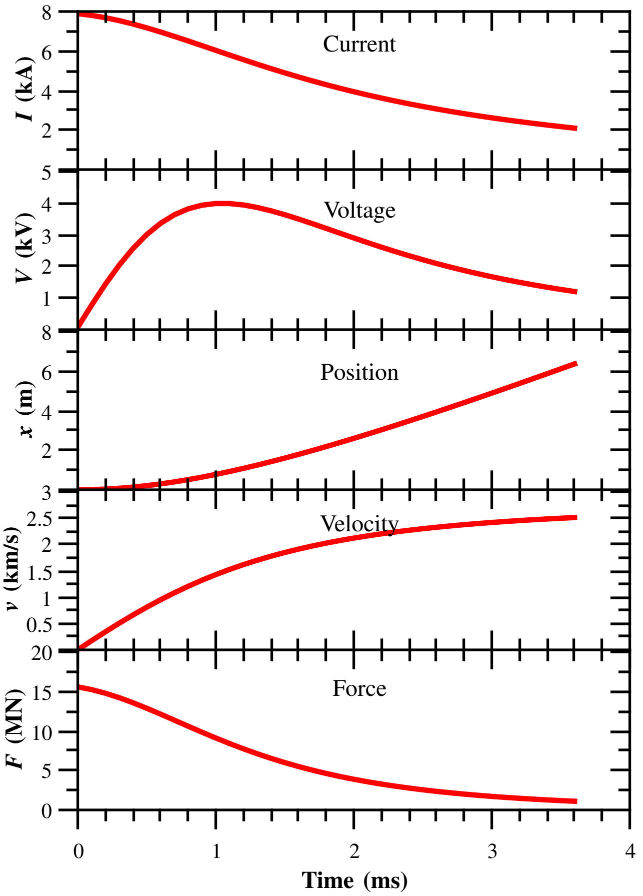

Fig. 2. Railgun simulation results for $W_0 = 66\,\mathrm{MJ}$, $\tau = 50\,ms$ and $L_{coil} = 2.12\mu\mathrm{H}$

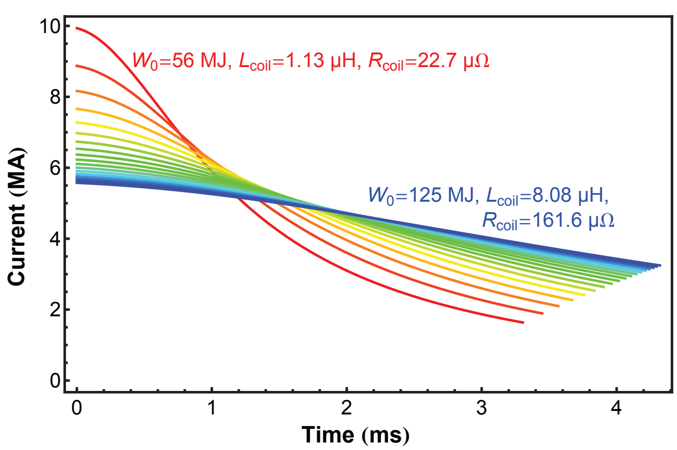

Fig. 3. Simulated current waveforms for different W_0 and L_{coil} but constant $\tau = 50\,\mathrm{ms}$. The curves are shown until the projectile leaves the bore

as

$$\eta = \frac{W_{kin}}{W_{mag}} = \frac{m \times v_{muzzle}^2}{(L_{coil} + L_w) \times I_0^2} \tag{5}$$

Because $I_0 \neq 0$ at $t = 0$, the initial energy in this model is also stored in the inductance of the cables which is expressed by L_w in eq. 5.

Figure 4 a illustrates how the transfer efficiency depends on the inductance and therefore, on the pulse shape. Each curve belongs to one time constant τ. It can be observed that better transfer efficiencies are possible with smaller inductances. Furthermore, increasing τ has a limited effect. The curve for $\tau = 5\,\mathrm{s}$ is covered by the curve for $\tau = 1\,\mathrm{s}$, for example.

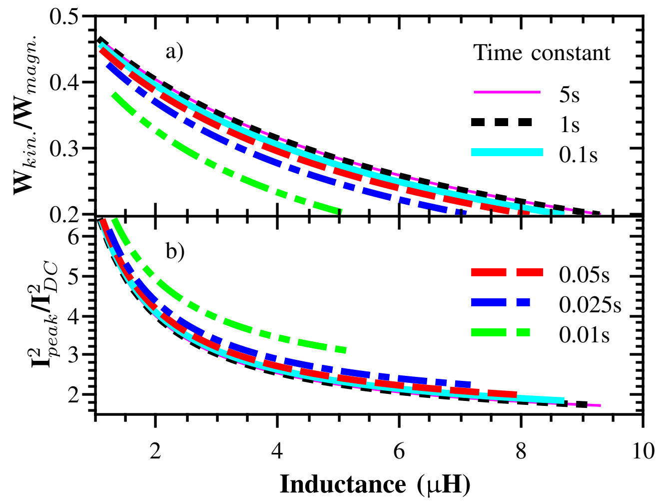

Fig. 4. Transfer efficiency (a) and peak to average force ratio (b), depending on the coil inductance and τ

In the railgun the magnetic stresses are proportional to I^2 (see eq. 2). Thus, Fig. 4 b shows the square of the peak current for the simulated solutions, depending on the coil inductance. The data are normalized by the direct current of 3.95 MA which is the current in case of constant acceleration [6]. Due to the normalization, the graph is equivalent to the electromagnetic forces and the magnetic pressure. Again, the color and shape of the curves depend on the time constant of the coil. It can be noticed that the maximum electromagnetic forces are larger at small inductances. Note that curves for a larger τ do overlap again.

IV. Discussion

As expected, the simulation shows that small inductances are propitious to the transfer efficiency (see Fig. 4). The explanation is given by Fig. 3. The bigger the inductance, the longer the pulse and the more energy is lost after the projectile has left the railgun barrel. This is a well-known relationship and valid as long as the remaining energy is not recovered. However, an important finding is that τ and hence the coil volume have a limited effect on the system efficiency.

The higher the efficiency, the higher the forces in the railgun, due to the increase in the initial current. This becomes clear by plotting Fig. 4 again with varied axes (see Fig. 5). Thus, the coil inductance cannot be chosen to be arbitrarily small. It needs to have a minimum value which depends on the maximum forces in the railgun. The forces depend on the caliber of the railgun as the maximum current is directly proportional to it. Assuming that the railgun can handle stresses which are 4 times as high as in the DC case, i.e. by increasing the caliber by a factor of 2, the operating conditions on the left of the dashed vertical line in Fig. 5 are possible. If an efficiency of 30 % or more is desired, the achievable operating conditions are limited to the part above

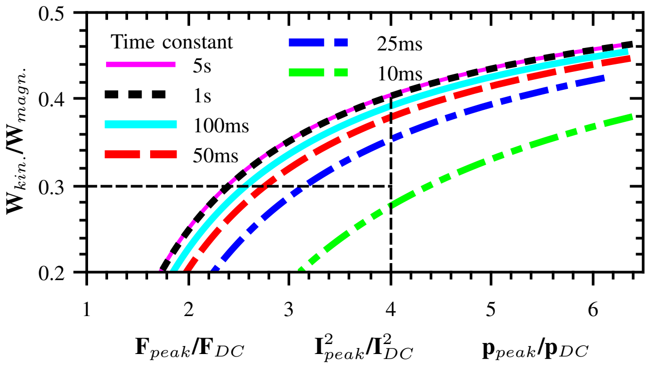

Fig. 5. Peak to average force ratio depending on transfer efficiency

the dashed horizontal line. The smallest coil possible has a τ of approximately 15 ms (point of intersection of the dashed lines in Fig. 5). The bigger τ, the better the efficiency but for $\tau > 1$ s, a further increase in the coil has no visible effect. Next, it follows from Fig. 4-b that the inductance needs to be > 2.2 µH for this case ($\tau = 15$ ms, $F_{peak}/F_{DC} = 4$).

Note that the magnetic forces in the coil are proportional to the energy stored for a given coil size (fixed τ) and decrease with an increasing τ.

V. Conclusion and Outlook

A numerical simulation of an inductively powered railgun was generated and validated by comparison with experimental results. A parametric study was conducted by varying the time constant of the coil, the initial energy and the initial current. The parametric study showed that the current pulse shape is responsible for the transfer efficiency and the maximum forces in the railgun and coil. A long pulse with a slow decay of the initial current is propitious to the generated forces. A short pulse with a high initial current leads to the best transfer efficiency as no energy would be lost if the current pulse decays to zero before the projectile leaves the railgun. The pulse shape can be controlled by the inductance of the storage coil. In order to obtain a high efficiency it should be as low as possible. To keep the forces small, the inductance needs to be big. Thus, the coil inductance should be chosen to be as small as possible without exceeding the allowed forces within the railgun. The time constant τ has a limited influence on the pulse shape in a railgun system and therefore, on the efficiency and the forces. Thus, the size of the storage coil with respect to an inductive power supply for a railgun is determined by other limitations like the heat dissipation or the tensile strength of the coil material rather than by the electrical characteristics within the railgun circuit. In future, further parameters influencing the design of the coil such as charging parameters, pulse repetition, and others will be investigated.

Acknowledgment

This work was supported by the French Government Defense procurement and technology agency (DGA) as part of the ANR Astrid program under Grant ANR-14-ASTR-0025.

References

[1] D. Hackworth, D. Deis, P. Eckels, and D. Marschik, "A 10 MJ cryogenic inductor," *IEEE Trans. Magn.*, vol. 22, no. 6, pp. 1495–1498, Nov. 1986.

[2] A. Pokryvailo, "Development of long-charge inductive storage systems at Soreq NRC," in *15th IEEE Int. Pulsed Power Conf. (PPPS). Dig. Techn. Pap.*, Monterey, US-CA, 2005, pp. 100–103.

[3] J. B. Cornette, J. D. Sterrett, J. R. Lippert, and R. W. Williams, "Final design and commissioning test results for the hypervelocity launcher research complex battery power supply," in *7th IEEE Int. Pulsed Power Conf. (PPPS). Dig. Techn. Pap.*, 1989, pp. 131–133.

[4] E. Spahn, M. Lichtenberger, and F. Hatterer, "Pulse forming network for the 10 MJ-railgun PEGASUS," in *Proc. 5th Europ. Symp. Electromagn. Launch Techn.*, Toulouse, France, Apr.10-13 1995.

[5] O. Liebfried and V. Brommer, "A four-stage XRAM generator as inductive pulsed power supply for a small-caliber railgun," *IEEE Trans. Plasma Sci.*, vol. 41, no. 10, pp. 2805–2809, Oct. 2013.

[6] S. Hundertmark and D. Lancelle, "A scenario for a future european shipboard railgun," *IEEE Trans. Plasma Sci.*, vol. 43, no. 5, pp. 1194–1197, May 2015.

[7] X. Liu, X. Yu, and X. Liu, "Performance analysis and parameter optimization of cpps-based electromagnetic railgun system," *IEEE Transactions on Plasma Science*, vol. 44, no. 3, pp. 281–288, March 2016.

[8] R. T. Meyer, R. A. DeCarlo, and J. Dickerson, "Energy transfer efficiency optimization in an electromagnetic railgun," *IEEE Transactions on Plasma Science*, vol. 45, no. 4, pp. 702–710, April 2017.

[9] S. Hundertmark and O. Liebfried, "Power supply options for a naval railgun," submitted to *IEEE Trans. Plasma Sci.*, 2017, arXiv:1709.05901.

[10] W. Ying, R. A. Marshall, and C. Shukang, *Physics of Electric Launch - EML Book 1*. Beijing, China: Science Press, 2004.

[11] F. J. Deadrick, R. S. Hawke, and J. D. Scudder, "MAGRAC - A railgun simulation program," *IEEE Trans. Magn.*, vol. 18, no. 1, pp. 94–104, Jan. 1982.